# Robust Flux and Speed State Observer Design for Sensorless Control of a Double Star Induction Motor

Mahmoud A. Mossa [1*], Houari Khouidmi [2], AlfianMa'arif [3]
[1] Electrical Engineering Department, Faculty of Engineering, Minia University, Minia 61111, Egypt
[2] Hassiba Benbouali University, Faculty of Technology 151 Hay Es-Salem Chlef 02000-Algeria
[3] Department of Electrical Engineering, Universitas Ahmad Dahlan, Yogyakarta 55191, Indonesia
Email: [1] mahmoud_a_mossa@mu.edu.eg, [2] h.khouidmi@univ-chlef.dz, [3] alfian.maarif@te.uad.ac.id
*Corresponding Author

***Abstract*—In this paper, a robust flux and speed observer for sensorless control of a double star induction motor is presented. Proper operation of vector control of the double star induction motor requires reliable information from the process to be controlled. This information can come from mechanical sensors (rotational speed, angular position). Furthermore, mechanical flux and speed sensors are generally expensive and fragile and affect the reliability of the system. However, the control without sensors must-have performance that does not deviate too much from that which we would have had with a mechanical sensor. In this framework, this work mainly deals with the estimation of the flux and speed using a robust state observer in view of sensorless vector control of the double star induction motor. The evaluation criteria are the static and dynamic performances of the system as well as the errors between the reference values and those estimated. Extensive simulation results and robustness tests are presented to evaluate the performance of the proposed sensorless control scheme. Furthermore, under the same test conditions, a detailed comparison between the proposed state observer and the sliding mode-MRAS technique is carried out where the results of its evaluation are investigated in terms of their speed and flux tracking capability during load and speed transients and also with parameter variation. It is worth mentioning that the proposed state observer can obtain both high current quality and low torque ripples, which show better performance than that in the MRAS system.**

***Keywords—State observer; Double star IM; Robustness; Sensorless control; Multiphase machines***

## I. INTRODUCTION

At high power, alternating current machines supplied by static converters are obtaining more attention to be utilized in different industrial applications. However, due to the constraints on the power components, the switching frequency and, consequently, the performance is limited. To allow the use of components with higher switching frequencies, the power must be segmented. To fulfill this need, one possible solution is to use machines with a large number of phases or multi-star machines. These polyphase machines appeared in 1969 [1, 2], offering an interesting alternative to relieving the stresses affecting both windings and switches. In fact, increasing the number of phases enables power splitting, resulting in a decrease in switching voltages at a given current. In addition, these machines additionally enable the mechanical load to filter through more readily by allowing the amplitude of torque ripples to be decreased and their frequency to be increased. At last, the multiplication of the number of phases increases the reliability by enabling one or more faulty phases to operate [3-6]. This type of machine constitutes an obvious potential and provides system designers with operation in degraded mode, which is most important in the fields of systems control [7-9]. Despite all these advantages, it is still very complicated to control compared to a DC machine because of its high nonlinear and coupled mathematical model [10] and certain variables, in particular the magnetic flux, are difficult to measure, and several parameters such as resistances, torque and inertia are likely to change very widely during operation [11].

Many traditional control methods, such as vector control and direct torque control, have been significantly tested in many research papers, especially on the double star induction machine, because of their advantages compared to other induction machines [12-14]. These methods have proven particularly efficient and successful in decoupling torque and magnetic flux, which encouraged us to support them with control algorithms that do not rely on mechanical sensors in an attempt to completely abandon them for their multiple drawbacks that directly affect the efficiency of the control system as a whole. Unfortunately, the aforementioned controls require knowledge of one of the stator or rotor fluxes, but the latter is not measurable [15-19]. This raises in many papers the problem of estimating or observing these quantities.

A search for simplicity of design and robustness becomes one of the most important criteria in many applications. This demand particularly mobilizes researchers [16, 18]. We strive above all to dispense the speed and flux sensors. They are the weak link in the control chain. Indeed, in addition to the size and the difficulty of adapting and mounting on all types of drive, it is fragile and expensive. We, therefore, try to have its function fulfilled by sensors of electrical quantities and calculation algorithms in order to reconstitute the speed and flux of the DSIM. With increasingly powerful digital computing resources, methods that were impossible to implement a few years ago are becoming feasible on low-cost DSPs [20, 21].

In practice, the state observer takes two different forms, a reduced order observer, where only the immeasurable state variables of the system are reconfigured [22-24], and a full order observer, for which all state variables of the system are reconfigured. The performance of this structure obviously depends on the choice of the gain matrix [25-29]. Unfortunately, rare studies in the literature were concerned with the sensorless operation of double star IM; some of them used the sliding mode observers [30], and others adopted the MRAS estimator [31, 32]. However, investigating the robustness of these observers against the uncertainties and disturbances was not fulfilled sufficiently.

Although the MRAS-based speed estimation method [32], which was applied to the DSIM engine, has many advantages, such as low computational complexity and easy implementation, its combination with sliding mode (SM) technology may make it a difficult method to implement due to some drawbacks, the most important of which is sensitivity uncertainty in the reference model, chattering problems and complexity in the design of the adaptive mechanism block and other drawbacks such as difficulty in adjusting parameters design, sensitivity to measurement noise, inaccuracy of estimating low speeds and durability considerations that may lead to destabilization of the system during different operating modes.

Following these requirements, the current study presents a detailed design for a robust flux and speed state observer for enhancing the reliability and robustness of the vector control applied to a double-star IM. Extensive evaluation tests for the observer's performance under different operating speeds, different loading conditions, and various system uncertainties are carried out to validate the design of the adopted observer. The results are discussed and analyzed in detail, illustrating the impact of each variable change on the observer dynamics.

The paper is structured such that Section 2 briefly introduces the double star induction motor (DSIM) model in (d, q) axes. Section 3 presents the design of the direct vector control method of DSIM. Subsequently, in Section 4, the speed and flux state observer design is discussed. At last, the complete control scheme illustrated in Fig. 1 is firstly implemented for numerical simulation to evaluate the performance of the proposed speed and flux state observer for sensorless vector control of DSIM, and then a comparison tests of the proposed state observer and SM-MRAS estimator proposed in [32] under the same conditions are investigated, and corresponding results are analyzed. Finally, the conclusions are summarized.

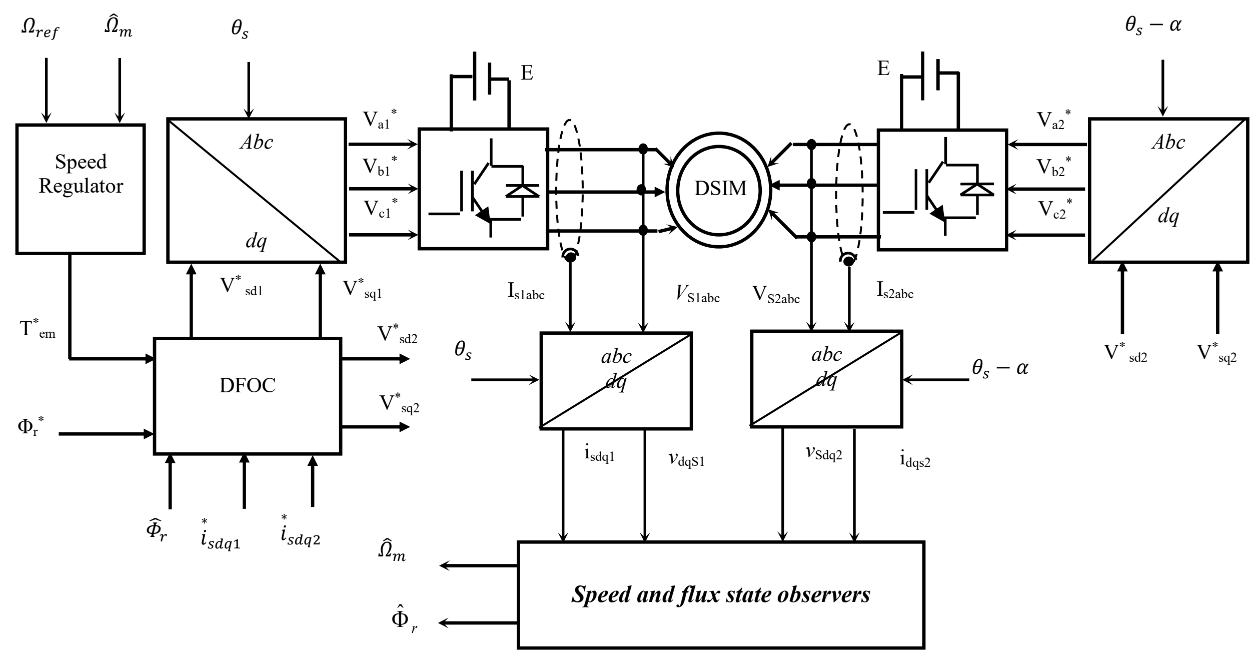


Fig. 1. Sensorless vector control scheme of DSIM

## II. MATHEMATICAL MODEL OF DSIM

If the assigned reference to the (d, q) axes is the rotating field, the equations of DSIM can be expressed as [21]:

### A. Voltages Equations

The d-q axis stators and rotor voltage equations are given by:

$$\begin{cases} v_{sd1} = R_{s1} i_{sd1} + \dfrac{d\Phi_{sd1}}{dt} - \omega_s \Phi_{sq1} \\ v_{sq1} = R_{s1} i_{sq1} + \dfrac{d\Phi_{sq1}}{dt} + \omega_s \Phi_{sd1} \\ v_{sd2} = R_{s2} i_{sd2} + \dfrac{d\Phi_{sd2}}{dt} - \omega_s \Phi_{sq2} \\ v_{sq2} = R_{s2} i_{sq2} + \dfrac{d\Phi_{sq2}}{dt} + \omega_s \Phi_{sd2} \\ 0 = R_r i_{rd} + \dfrac{d\Phi_{rd}}{dt} - (\omega_s - \omega_m)\Phi_{rq} \\ 0 = R_r i_{rq} + \dfrac{d\Phi_{rq}}{dt} + (\omega_s - \omega_m)\Phi_{rd} \end{cases} \quad (1)$$

Where $v_{sdq1}$, $v_{sdq2}$ is first and second voltages in the stator frame. $i_{sdq1}$, $i_{sdq2}$ is first and second currents in the stator frame. $\Phi_{sdq1}, \Phi_{sdq2}$ is the first and second stator flux in the stator frame. $\Phi_{rdq}$ is Rotor flux referred to as stator frame. $\omega_s$, $\omega_m$ is Stator and rotor angular frequencies. $R_{s1,2}$, $R_r$ is the first and second stator and rotor resistances.

*B. Flux Equations*

The stators and rotor flux can be expressed in terms of stators and rotor current as:

$$\begin{cases} \Phi_{sd1} = L_{s1} i_{sd1} + L_m(i_{sd1} + i_{sd2} + i_{rd}) \\ \Phi_{sq1} = L_{s1} i_{sq1} + L_m(i_{sq1} + i_{sq2} + i_{rq}) \\ \Phi_{sd2} = L_{s2} i_{sd2} + L_m(i_{sd1} + i_{sd2} + i_{rd}) \\ \Phi_{sq2} = L_{s2} i_{sq2} + L_m(i_{sq1} + i_{sq2} + i_{rq}) \\ \Phi_{rd} = L_r i_{rd} + L_m(i_{sd1} + i_{sd2} + i_{rd}) \\ \Phi_{rq} = L_r i_{rq} + L_m(i_{sq1} + i_{sq2} + i_{rq}) \end{cases} \quad (2)$$

Where $L_{s1,2}$ is First and second stator inductances, $L_r$ is Rotor inductance and $L_m$ is Magnetizing inductance.

The substitution of (2) in (1) develops the mathematical model of DSIM as following

$$\begin{cases} \dfrac{di_{sd1}}{dt} = \dfrac{1}{\sigma(L_{s1}+L_m)} \left[ \begin{array}{l} V_{sd1} - R_{s1} i_{sd1} - \dfrac{L_m L_r}{L_m + L_r}\dfrac{di_{sd2}}{dt} - \dfrac{L_m}{L_m+L_r}\dfrac{d\Phi_{rd}}{dt} + \\ +\omega_s\left( (L_{s1}+L_m)\sigma i_{sq1} + \dfrac{L_m L_r}{L_m+L_r} i_{sq2} + \dfrac{L_m}{L_m+L_r}\Phi_{rq} \right) \end{array} \right] \\ \dfrac{di_{sq1}}{dt} = \dfrac{1}{\sigma(L_{s1}+L_m)} \left[ \begin{array}{l} V_{sq1} - R_{s1} i_{sq1} - \dfrac{L_m L_r}{L_m + L_r}\dfrac{di_{sq2}}{dt} - \dfrac{L_m}{L_m+L_r}\dfrac{d\Phi_{qr}}{dt} + \\ -\omega_s\left( (L_{s1}+L_m)\sigma i_{sd1} + \dfrac{L_m L_r}{L_m+L_r} i_{sd2} + \dfrac{L_m}{L_m+L_r}\Phi_{rd} \right) \end{array} \right] \\ \dfrac{di_{sd2}}{dt} = \dfrac{1}{\sigma(L_{s2}+L_m)} \left[ \begin{array}{l} V_{sd2} - R_{s2} i_{ds2} - \dfrac{L_m L_r}{L_m + L_r}\dfrac{di_{sd1}}{dt} - \dfrac{L_m}{L_m+L_r}\dfrac{d\Phi_{rd}}{dt} + \\ +\omega_s\left( (L_{s2}+L_m)\sigma i_{sq2} + \dfrac{L_m L_r}{L_m+L_r} i_{sq1} + \dfrac{L_m}{L_m+L_r}\Phi_{rq} \right) \end{array} \right] \\ \dfrac{di_{sq2}}{dt} = \dfrac{1}{\sigma(L_{s2}+L_m)} \left[ \begin{array}{l} V_{sq2} - R_{s2} i_{sq2} - \dfrac{L_m L_r}{L_m + L_r}\dfrac{di_{sq1}}{dt} - \dfrac{L_m}{L_m+L_r}\dfrac{d\Phi_{rq}}{dt} + \\ -\omega_s\left( (L_{s2}+L_m)\sigma i_{sd2} + \dfrac{L_m L_r}{L_m+L_r} i_{sd1} + \dfrac{L_m}{L_m+L_r}\Phi_{rd} \right) \end{array} \right] \\ \dfrac{d\Phi_{rd}}{dt} = \dfrac{L_m}{T_r}(i_{sd1}+i_{sd2}) - \dfrac{1}{T_r}\Phi_{rd} - (\omega_s - \omega_m)\Phi_{rq} \\ \dfrac{d\Phi_{rq}}{dt} = \dfrac{L_m}{T_r}(i_{sq1}+i_{sq2}) - \dfrac{1}{T_r}\Phi_{rq} + (\omega_s - \omega_m)\Phi_{rd} \end{cases} \quad (3)$$

With

$$\sigma = 1 - \frac{L_m^2}{(L_m+L_r)(L_m+L_s)}, L_{s1} = L_{s2} = L_s, T_r = \frac{L_m + L_r}{R_r}$$

Where $\sigma$ is the total leakage factor and $T_r$ is rotor time constant.

## III. DIRECT VECTOR CONTROL OF DSIM

In this method, it is important to note that a flux estimation step is necessary. Then, calculate the flux modulus and its phase from easily measurable variables like currents and voltages.

The rotor flux components can then be expressed utilizing (3) as follows

$$\begin{cases} \Phi_{rd} = \int \left[ \dfrac{L_m}{T_r}(I_{sd1} + I_{sd2}) - \dfrac{1}{T_r}\Phi_{rd} - \omega_r \Phi_{rq} \right] dt \\ \Phi_{rq} = \int \left[ \dfrac{L_m}{T_r}(I_{sq1} + I_{sq2}) - \dfrac{1}{T_r}\Phi_{rq} + \omega_r \Phi_{rd} \right] dt \end{cases} \quad (4)$$

The principle of the rotor flux orientation gives [4, 15] as

$$\begin{cases} \Phi_r = \Phi_{rd} \\ \Phi_{rq} = 0 \end{cases} \quad (5)$$

The rotor flux and electromagnetic torque expressions of the DSIM can be presented by

$$\begin{cases} \dfrac{d\Phi^*{}_r}{dt} = \dfrac{1}{T_r}[L_m(i^*{}_{sd1} + i^*{}_{sd2}) - \Phi^*{}_r] \\ T^*{}_{em} = p\dfrac{L_m}{L_m + L_r}[(i^*{}_{sq1} + i^*{}_{sq2})\Phi^*{}_r] \end{cases} \quad (6)$$

The Laplace transformation of (6) gives as

$$\begin{cases} \Phi^*{}_r = \dfrac{L_m}{1+T_r s}\left(i^*{}_{sd1} + i^*{}_{sd2}\right) \\ T^*{}_{em} = p\dfrac{L_m}{L_m+L_r}\left[\left(i^*{}_{sq1} + i^*{}_{sq2}\right)\Phi^*{}_r\right] \end{cases} \tag{7}$$

Because the DSIM stators are similar, then the stators currents provided by these two identical stators are the same, thus

$$\begin{cases} i^*{}_{sd1} = i^*{}_{sd2} = \dfrac{1+T_r s}{2L_m}\Phi^*{}_r \\ i^*{}_{sq1} = i^*{}_{sq2} = p\dfrac{L_m+L_r}{2L_m\Phi^*{}_r}T^*{}_{em} \end{cases} \tag{8}$$

From DSIM model (3) and references currents equation (8), the references control voltages $V^*_{sd1}$, $V^*_{sq1}$, $V^*_{sd2}$ are

$$\begin{cases} V^*{}_{sd1} = \sigma(L_{s1}+L_m)\dfrac{di^*{}_{sd1}}{dt} - R_{s1}i^*{}_{sd1} - \omega_s\left((L_{s1}+L_m)\sigma i^*{}_{sq1} + \dfrac{L_mL_r}{L_m+L_r}i^*{}_{sq2}\right) \\ V^*{}_{sq1} = \sigma(L_{s1}+L_m)\dfrac{di^*{}_{sq1}}{dt} - R_{s1}i^*{}_{sq1} + \omega_s\left((L_{s1}+L_m)\sigma i^*{}_{sd1} + \dfrac{L_m}{L_m+L_r}\Phi^*{}_r\right) \\ V^*{}_{sd2} = \sigma(L_{s2}+L_m)\dfrac{di^*{}_{sd2}}{dt} - R_{s2}i^*{}_{ds2} - \omega_s\left((L_{s2}+L_m)\sigma i^*{}_{sq2} + \dfrac{L_mL_r}{L_m+L_r}i^*{}_{sq1}\right) \\ V^*{}_{sq2} = \sigma(L_{s2}+L_m)\dfrac{di^*{}_{sq2}}{dt} - R_{s2}i^*{}_{sq2} + \omega_s\left((L_{s2}+L_m)\sigma i^*{}_{sd2} + \dfrac{L_m}{L_m+L_r}\Phi^*{}_r\right) \end{cases} \tag{9}$$

## IV. Flux and Speed State Observers of DSIM

An observer (Fig. 2) proper is an estimator having an additional input $G(Y-\hat{Y})$. This additional input ensures the operation in a closed loop and, therefore, the stability of the reconstitution.

In order to know well the principle of an observer, it is supposed that the studied system is described by the equation (10).

$$\begin{cases} \dfrac{dX}{dt} = AX + BU \\ Y = CX \end{cases} \tag{10}$$

Where for any time, X∈$\Re^n$, U∈$\Re^m$, and Y∈$\Re^l$ respectively express the state vector, the input vector, and the output vector of the system. A∈$\Re^{n\times n}$ is the non-stationary transition matrix, as it depends on the estimated variable, B∈$\Re^{n\times m}$is the input matrix of the system and C∈$\Re^{l\times n}$ is the output matrix. These matrices (A, B, and C) are directly calculated from the operating equations of the system.

Some command methods do not necessarily require reformulating the entire state of the system. Indeed, according to the case studies, only part of the state must be estimated to satisfy the needs. The reduced order observer introduced by Luenberger [22] consists in estimating non-measurable states. Thus, for a system defined by (10), the reduced observer will be of order n-l.

The electric equations are linear in the states but depend on the mechanical speed $\omega_m$, one can construct a reduced order state observer of the Luenberger type [12, 17], obtained from the representation of the complete state of the DSIM in the frame (d, q) or (α, β).

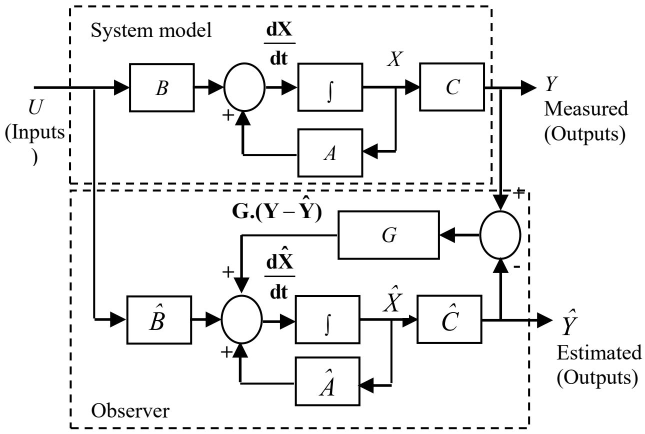


Fig. 2. State space form of an observer

The complete state representation in the frame (d, q) which will be used to design our observers will therefore be the following:

$$\begin{cases} \dfrac{dX}{dt} = A(\omega_m)X + BU \\ Y = CX \end{cases} \tag{11}$$

where

$$X = [I_{ds1}+I_{ds2} \quad I_{qs1}+I_{qs2} \quad \Phi_{dr} \quad \Phi_{qr}]^T$$

and

$$U = [V_{ds1}+V_{ds2} \quad V_{qs1}+V_{qs2}]^T$$

$$A(\omega_m) = \begin{bmatrix} -\gamma\mu & \omega_s & \dfrac{K\mu}{Tr} & K\mu\omega_m \\ -\omega_s & -\gamma\mu & -K\mu\omega_m & \dfrac{K\mu}{Tr} \\ \dfrac{L_m}{Tr} & 0 & \dfrac{-1}{Tr} & -\omega_m \\ 0 & \dfrac{L_m}{Tr} & \omega_m & \dfrac{-1}{Tr} \end{bmatrix}$$

and

$$B = \begin{bmatrix} \dfrac{\mu}{\sigma(L_s+L_m)} & 0 \\ 0 & \dfrac{\mu}{\sigma(L_s+L_m)} \\ 0 & 0 \\ 0 & 0 \end{bmatrix}$$

$$C = \begin{bmatrix} 1 & 0 & 0 & 0 \\ 0 & 1 & 0 & 0 \end{bmatrix}$$

With

$$\sigma = 1 - \frac{L_m^2}{(L_m+L_r)(L_m+L_s)}, \mu = \frac{\sigma(L_m+L_r)(L_m+L_s)}{\sigma(L_m+L_r)(L_m+L_s)+L_mL_r}$$

$$K = \frac{2L_m}{\sigma(L_m+L_r)(L_m+L_s)}, \gamma = \frac{R_s}{\sigma(L_m+L_s)} + \frac{2R_rL_m^2}{\sigma(L_m+L_s)(L_m+L_r)^2}$$

The principle of construction, therefore, consists in correcting the dynamics of the estimate by considering the error between the real output and the reconstructed output, so an observer is a copy of the original system with an additional gain term. It is described as follows:

$$\begin{cases}\dfrac{d\hat{X}}{dt} = A(\omega_m).\hat{X} + BU + G\big(Y - C\hat{X}\big) \\ \hat{Y} = C\hat{X}\end{cases} \quad (12)$$

where $G$ is the observer gain matrix.

In order to reduce the complexity of the observer, we have to reduce the order of the state vector by choice of quantities to be observed.

To observe the rotor flux and the mechanical speed, considering the stator currents as inputs:

$$\begin{cases}\dfrac{d\hat{X}_\Phi}{dt} = A(\widehat{\omega}_m).\hat{X}_\Phi + B_I U_I \\ \hat{Y}_\Phi = \hat{X}_\Phi\end{cases} \quad (13)$$

where

$$\hat{X}_\Phi = \begin{bmatrix}\widehat{\Phi}_{dr} & \widehat{\Phi}_{qr}\end{bmatrix}^T$$

and

$$U_I = [I_{ds1} + I_{ds2} \quad I_{qs1} + I_{qs2}]^T$$

$$A(\widehat{\omega}_m) = \begin{bmatrix}\dfrac{-1}{\hat{T}_r} & -\widehat{\omega}_m \\ \widehat{\omega}_m & \dfrac{-1}{\hat{T}_r}\end{bmatrix}$$

and

$$B_I = \begin{bmatrix}\dfrac{L_m}{T_r} & 0 \\ 0 & \dfrac{L_m}{T_r}\end{bmatrix}$$

The observed stator currents are given by

$$\begin{cases}\dfrac{d\hat{X}_I}{dt} = A.\hat{X}_I + B_V U_V + K\mu[\psi] \\ \hat{Y}_I = \hat{X}_I\end{cases} \quad (14)$$

where

$$\hat{X}_I = \begin{bmatrix}\hat{I}_{ds1} + \hat{I}_{ds2} & \hat{I}_{qs1} + \hat{I}_{qs2}\end{bmatrix}^T$$

and

$$X_I = [I_{ds1} + I_{ds2} \quad I_{qs1} + I_{qs2}]^T$$

$$U_V = [V_{ds1} + V_{ds2} \quad V_{qs1} + V_{qs2}]^T$$

and

$$A = \begin{bmatrix}-\gamma\mu & \omega_s \\ -\omega_s & -\gamma\mu\end{bmatrix}$$

$$B_V = \begin{bmatrix}\dfrac{\mu}{\sigma(L_s + L_m)} & 0 \\ 0 & \dfrac{\mu}{\sigma(L_s + L_m)}\end{bmatrix}$$

and

$$[\psi] = \begin{bmatrix}\psi_{dr} \\ \psi_{qr}\end{bmatrix} = G(X_I - \hat{X}_I)$$

The flux observer (15) is obtained from equations (13) and (14):

$$\begin{cases}\dfrac{d\hat{X}_\Phi}{dt} = G(\hat{X}_I - X_I) + B_I U_I \\ \hat{Y}_\Phi = \hat{X}_\Phi\end{cases} \quad (15)$$

Comparing the observer equation (13) and (15) gives:

$$G(\hat{X}_I - X_I) = A(\widehat{\omega}_m).\hat{X}_\Phi \quad (16)$$

where

$$A(\widehat{\omega}_m) = \begin{bmatrix}\dfrac{1}{\hat{T}_r} & \widehat{\omega}_m \\ -\widehat{\omega}_m & \dfrac{1}{\hat{T}_r}\end{bmatrix}$$

and

$$\hat{X}_I - X_I = \begin{bmatrix}\tilde{\imath}_{ds} \\ \tilde{\imath}_{qs}\end{bmatrix}$$

The calculation of the observed speed leads to the following relation (17)

$$\widehat{\omega}_m = \frac{1}{\Phi_{dr}^2 + \Phi_{qr}^2}\left[\widehat{\Phi}_{dr}\hat{\psi}_{qr} - \widehat{\Phi}_{qr}\hat{\psi}_{dr}\right] \quad (17)$$

We finally deduce

$$\widehat{\omega}_m = \frac{1}{\Phi_{dr}^2 + \Phi_{qr}^2}\left[\widehat{\Phi}_{dr}G_1\big(\tilde{\imath}_{qs}\big) - \widehat{\Phi}_{qr}G_2(\tilde{\imath}_{ds})\right] \quad (18)$$

where

$$\tilde{\imath}_{ds} = (\hat{I}_{ds1} + \hat{I}_{ds2}) - (I_{ds1} + I_{ds2})$$
$$\tilde{\imath}_{qs} = (\hat{I}_{qs1} + \hat{I}_{qs2}) - (I_{qs1} + I_{qs2})$$

where G1 and G2 are the observer gains.

In order to have good performance, we chose the observer gains, which give a faster observer response than the system. On the other hand, a much faster choice of gains leads to sensitivity with respect to parametric variations.

## V. Test Results

In this section, to investigate the validity and robustness of the proposed sensorless vector control of DSIM based on a speed and flux state observer provided in Fig. 1, simulation tests are performed and done via the MATLAB/Simulink® platform. The values of the state observer gains used in the simulations are chosen after several adjustment tests ($G_1 = 1.2$, $G_2 = 1.8$).

For a fair comparison, the effectiveness of the proposed state observer is verified through the comparisons with the MRAS estimator presented in [32], where the simulation tests results are reproduced with the conditions of the same test for both methods in terms of their speed and flux tracking capability during load and speed transients and also with parameter variation.

The simulations are made for a nominal speed step of +280 rd/s and for a nominal load torque of 14 Nm applied at time t=1.5s and rejected at time t=2.5s. After that and at time t=3.5s, the speed is reversed at the same nominal value (-280rad/s).

The steady-state and speed reversal performance in the range of whole speed for both the proposed state observer and SM-MRAS estimator is shown in Fig. 3(a) and Fig. 3(b). The observed variables are real and estimated rotor speed, real and estimated rotor flux, electromagnetic torque, and stator phase current, respectively. The analysis of the responses shows perfect trajectory tracking. We observe an excellent estimation of speed and flux with negligible error and with very good precision. Furthermore, both state observer and SM-MRAS methods track the torque reference and show a very good dynamic performance. Regarding the performance of a torque step, rotor flux and stators phase currents response, torque and flux ripple, and currents THD are further evaluated for comparison. However, the results clearly indicate that the proposed state observer can confirm the quality of the obtained results compared to the SM-MRAS estimator, especially in terms of their speed and flux tracking, load rejection, and torque ripple.

Since the parameters of the DSIM are often linked to the operating conditions of the machine (heating, variation of the load, a saturation of the magnetic circuits, the shape of the air gap, skin effect, etc.), for this, we thought it would be more appropriate to test the influence of a possible parameter error on the proposed state observer and compared with SM-MRAS estimator proposed in [32].

In the simulation, an approach to these disturbances consists in introducing, at a given moment in the model of the DSIM, a parametric variation. This test mainly depends on changing the parameters of DSIM separately at times 1.5s to 2.5s.

Figs. 4(a, b) to Figs. 9(a, b) present respectively for both state observer and MRAS estimator, the speed and rotor flux responses for a variation of +50% of the rotor resistance, +50% of the stator resistances, and -50% decrease in the mutual inductance separately for a references speed of 150 rad/s and of 30rad/s for a low-speed test. We also note that the speed, as well as the rotor flux, is slightly affected by these variations, especially in low-speed tests for the MRAS estimator more than for the state observer, which confirms the capability of the proposed observer in maintaining the robustness of the control system.

In Figs.10(a, b) and Figs. 11(a, b), we notice that an increase of +100% of the inertia has an influence on the adjustment performance for high speeds than for low speeds. Indeed, we observe a considerable increase in the speed response time with a small overshoot during start-up and when reversing the speed. However, the decoupling phenomenon is guaranteed, and the speed, flux, and torque tracking are still ensured, especially in low-speed tests for the proposed state observer, which emphasize the validation of the designed state observer for the DSIM.

For performance comparison of the test results, the torque and flux ripples and the THD for the stator currents are introduced and evaluated in Table I.

TABLE I. PERFORMANCES EVALUATION OF THE STATE OBSERVER AND SM-MRAS ESTIMATOR

| Criterion | State Observer | SM-MRAS [32] |
|---|---|---|
| % Torque ripple | 24.53% | 49.62% |
| % Flux ripple | 22.24% | 23.08% |
| % Currents THD | 7.78% | 8.44% |

The ripples of torque and rotor flux are defined as

$$\%T_{ripple} = \frac{T_{\max} - T_{\min}}{T_{avg}}.100 \tag{19a}$$

$$\%\Phi_{ripple} = \frac{\Phi_{\max} - \Phi_{\min}}{\Phi_{avg}}.100 \tag{19b}$$

where $T_{max}$, $\Phi_{max}$ is the maximum torque and flux; $T_{min}$, $\Phi_{min}$ is the minimum torque and flux; $T_{avg}$, $\Phi_{avg}$ is the average torque and flux values, respectively.

The THD of stators phase currents is calculated by:

$$\%THD = \frac{\sqrt{I_2^2 + I_2^2 + \ldots + I_n^2}}{I_F} 100 \tag{20}$$

where $I_n$ is the root mean square (RMS) value of the harmonic $n$, $I_F$ is the RMS value of the fundamental current.

In terms of torque ripple, it shows that the torque ripple value of MRAS is more than twice the value of the state observer, namely, 49.62% versus 24.53%, respectively. With regard to flux ripple and currents THD, it shows that MRAS and state observer have very close flux ripple values with 23.08% and 22.24%, and very close THD values with 8.44% versus 7.78%, respectively.

## VI. CONCLUSION

In this paper, a speed and flux state observer for sensorless vector control of DSIM has been designed in detail. The simulation results allowed us to conclude that the sensorless vector control of the DSIM equipped with the designed flux and speed state observer provides satisfactory robustness against uncertainties, external disturbances, and speed change as well. Based on the investigation of the above simulation test results, it can be concluded that the state observer overcomes the drawback of a large torque ripple occurring in the MRAS estimator and has better robustness in low-speed tests. And meanwhile, the adopted sensorless vector control scheme-based state observer is also characterized by its simplicity of design and, in particular, by getting rid of the flux and speed sensors which represent the weak point of the feedback control chain. As a possible future work, the presented state observer can be utilized and tested with other configurations of multi-phase machines after considering the structure of each type.

## APPENDIX

### DOUBLE STAR INDUCTION MOTOR PARAMETERS

$P_n$=4.5kW, $f$=50Hz, $V_{n(\Delta/Y)}$=220/380V, $I_{n(\Delta/Y)}$=6.5A, $\Omega_n$=2751rpm, $p$=1, $R_{s1}$= $R_{s2}$=3.72Ω, $R_r$ =2.12Ω, $L_{s1}$= $L_{s2}$= 0.022H, $L_r$ = 0.006H, $L_m$ =0.3672H, $J$ =0.0625Kgm$^2$, $K_f$ =0.001Nm(rad/s)$^{-1}$

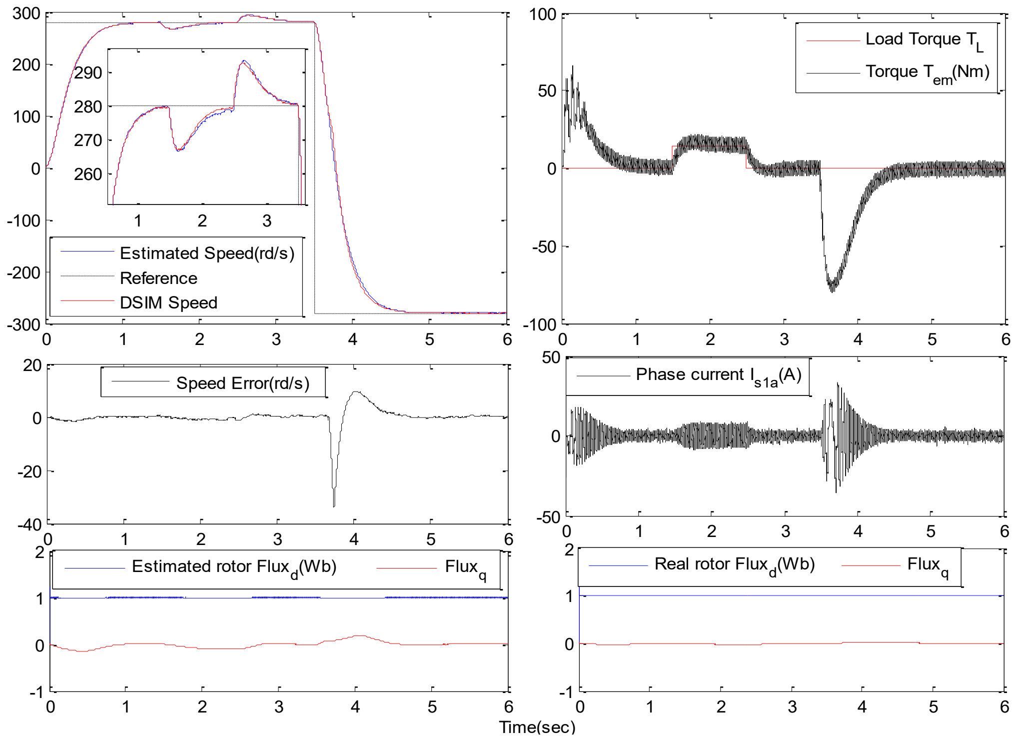


(a)

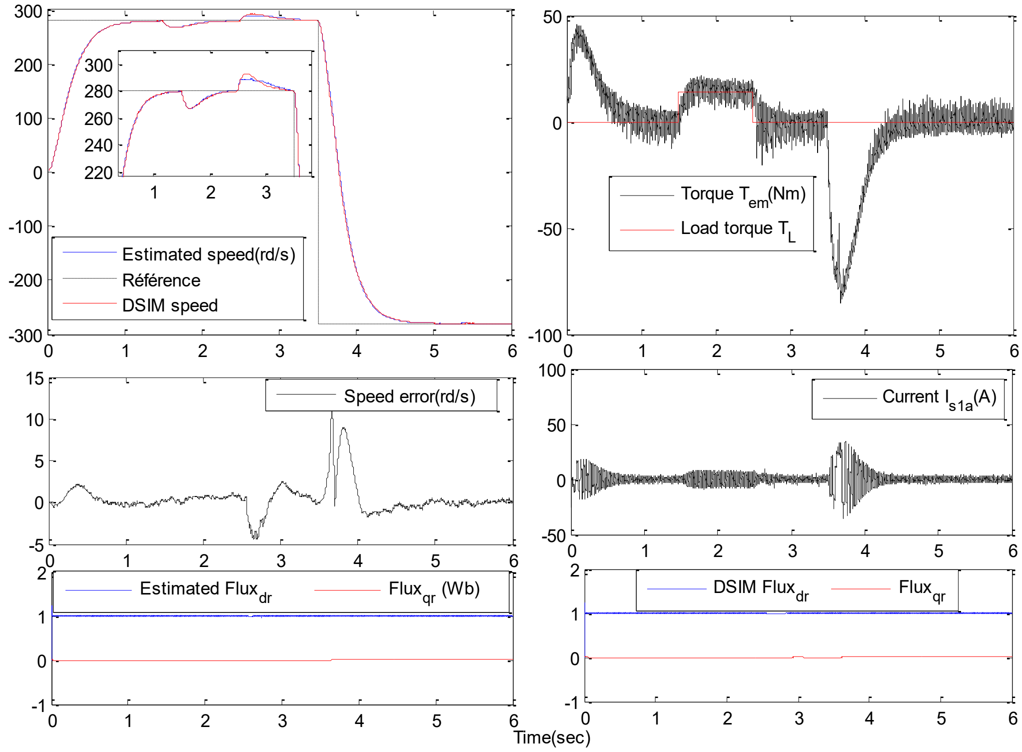


(b)

Fig. 3. Simulation results for sensorless direct vector control of DSIM. (a) proposed state observer. (b) SM-MRAS estimator [32].

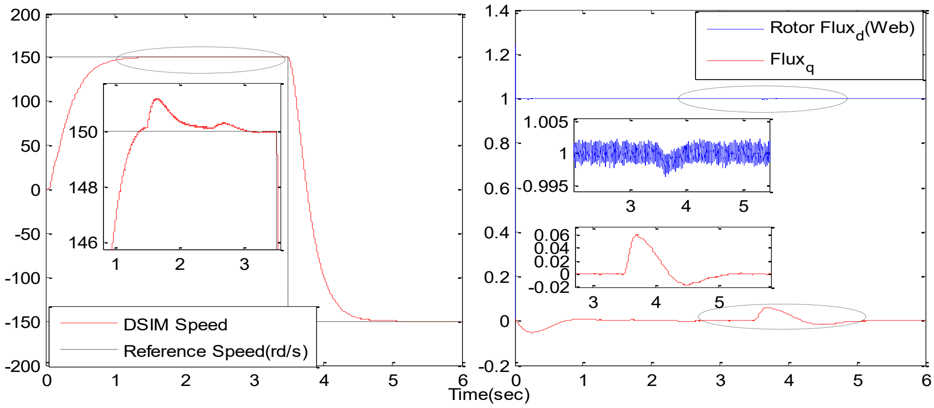


(a)

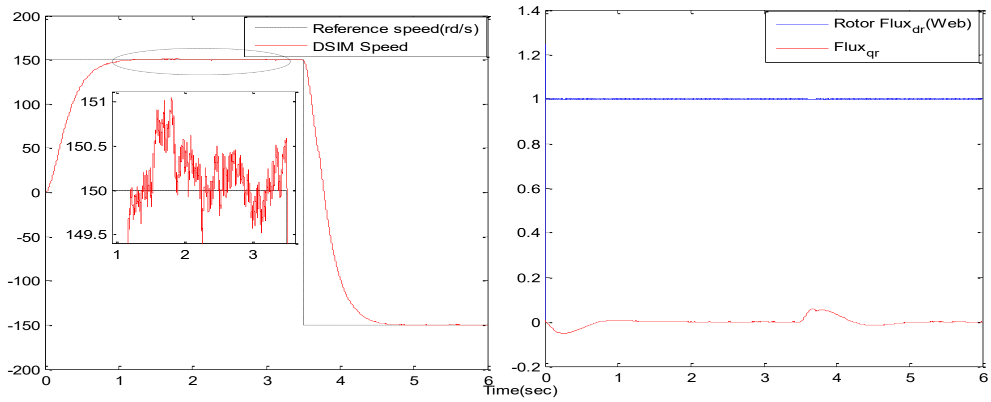


(b)

Fig. 4. Parameter variation of +50%Rr; for nominal speed test. (a) proposed state observer. (b) SM-MRAS estimator [32].

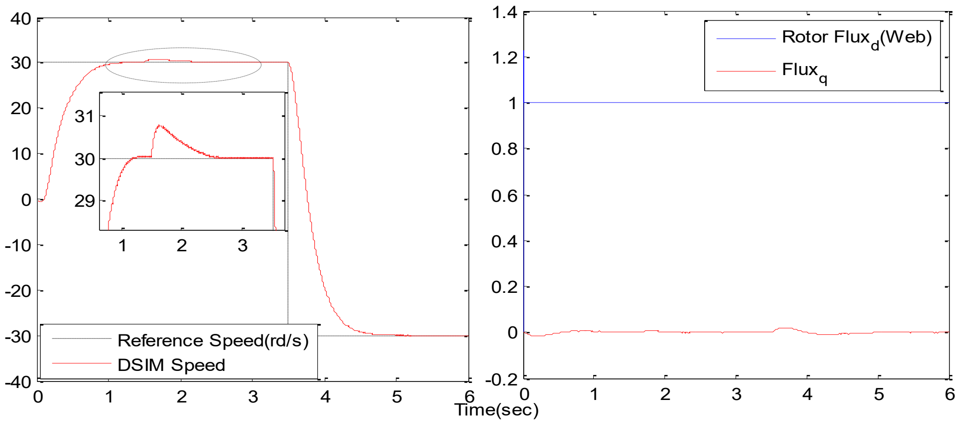


(a)

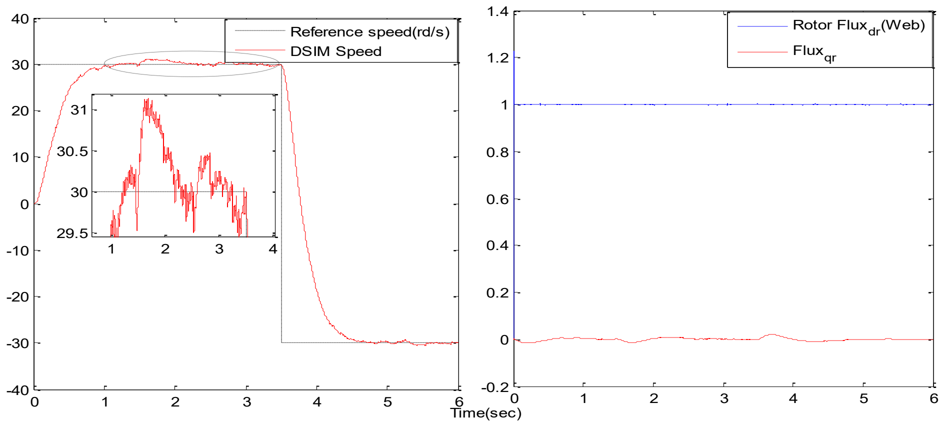


(b)

Fig. 5. Parameter variation of +50%Rr; for a low-speed test (a) proposed state observer (b) SM-MRAS estimator [32].

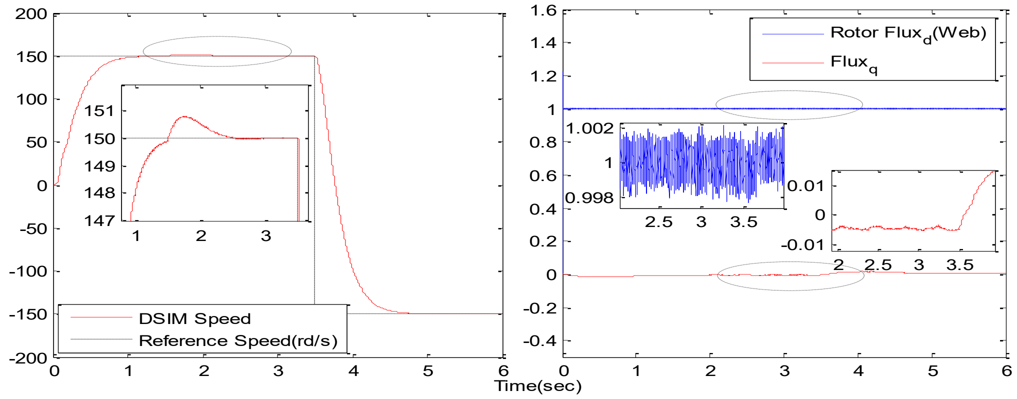


(a)

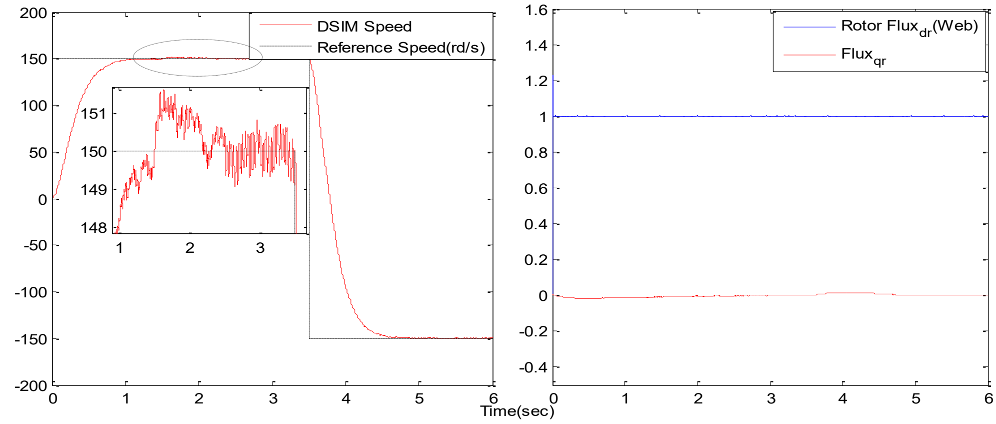


(b)

Fig. 6. Parameter variation of +50% $R_{s1,2}$; for nominal speed test. (a) proposed state observer. (b) SM-MRAS estimator [32].

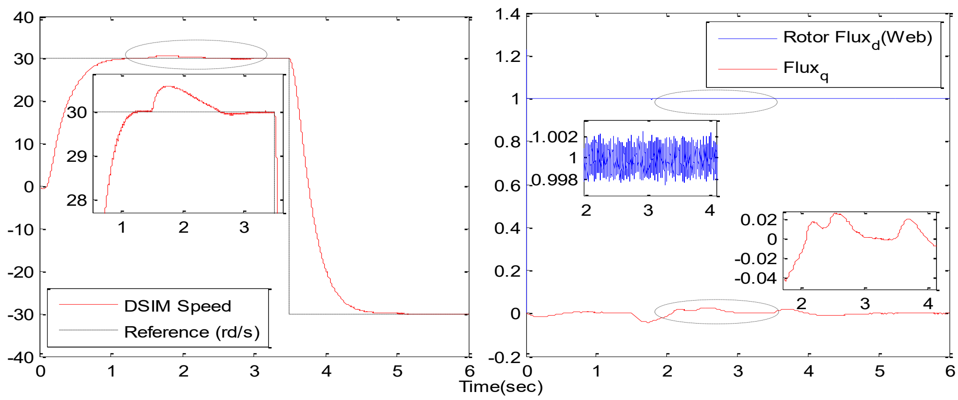


(a)

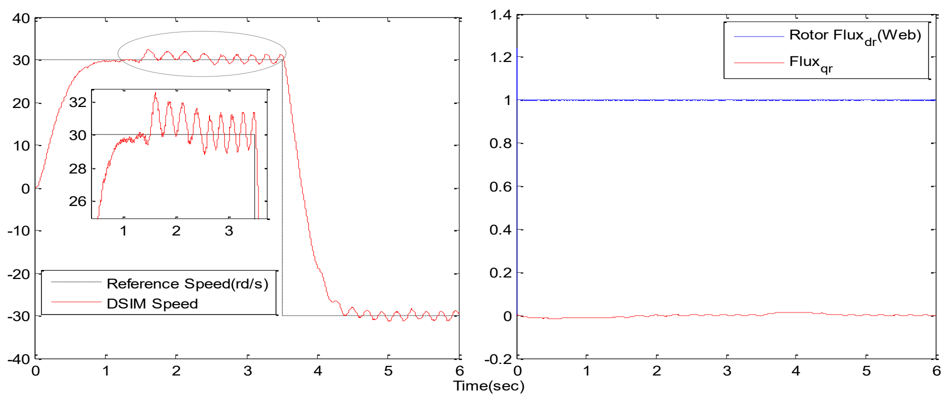


(b)

Fig. 7. Parameter variation of +50% $R_{s1,2}$; for low-speed test. (a) proposed state observer. (b) SM-MRAS estimator [32].

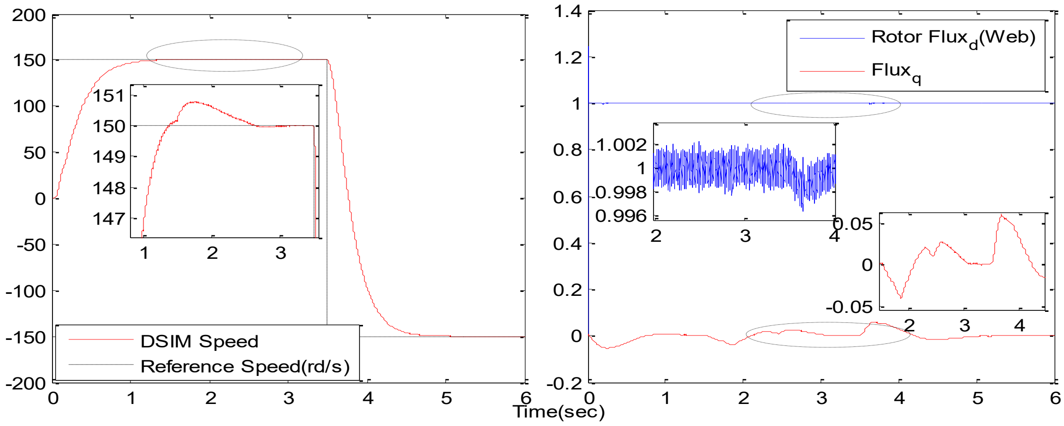

(a)

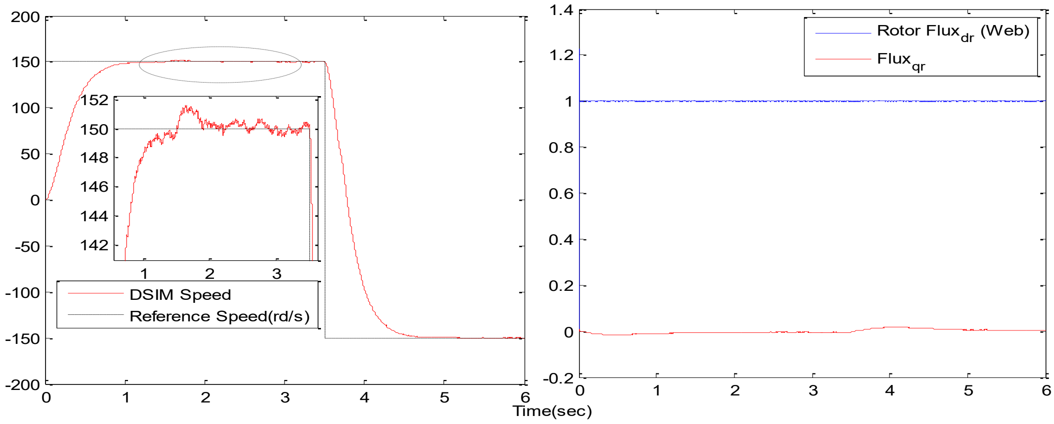

(b)

Fig. 8. Parameter variation of -50% Lm; for nominal speed test (a) proposed state observer (b) SM-MRAS estimator [32].

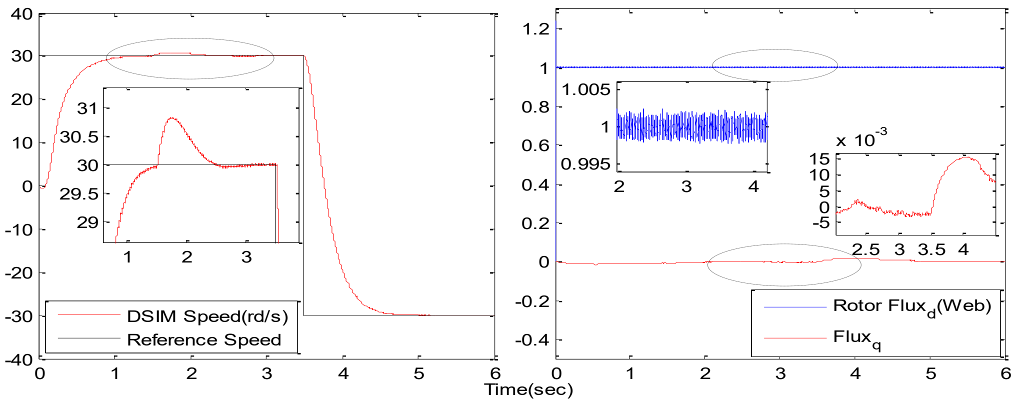

(a)

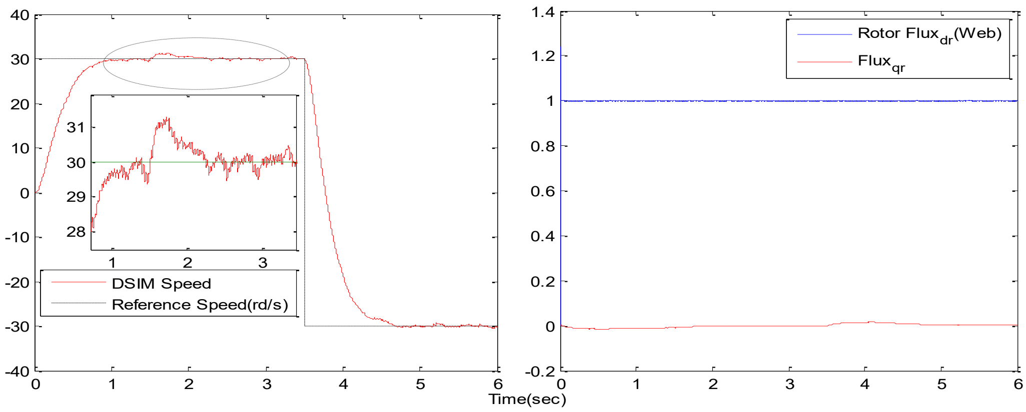

(b)

Fig. 9. Parameter variation of -50% Lm; for a low-speed test (a) proposed state observer (b) SM-MRAS estimator [32].

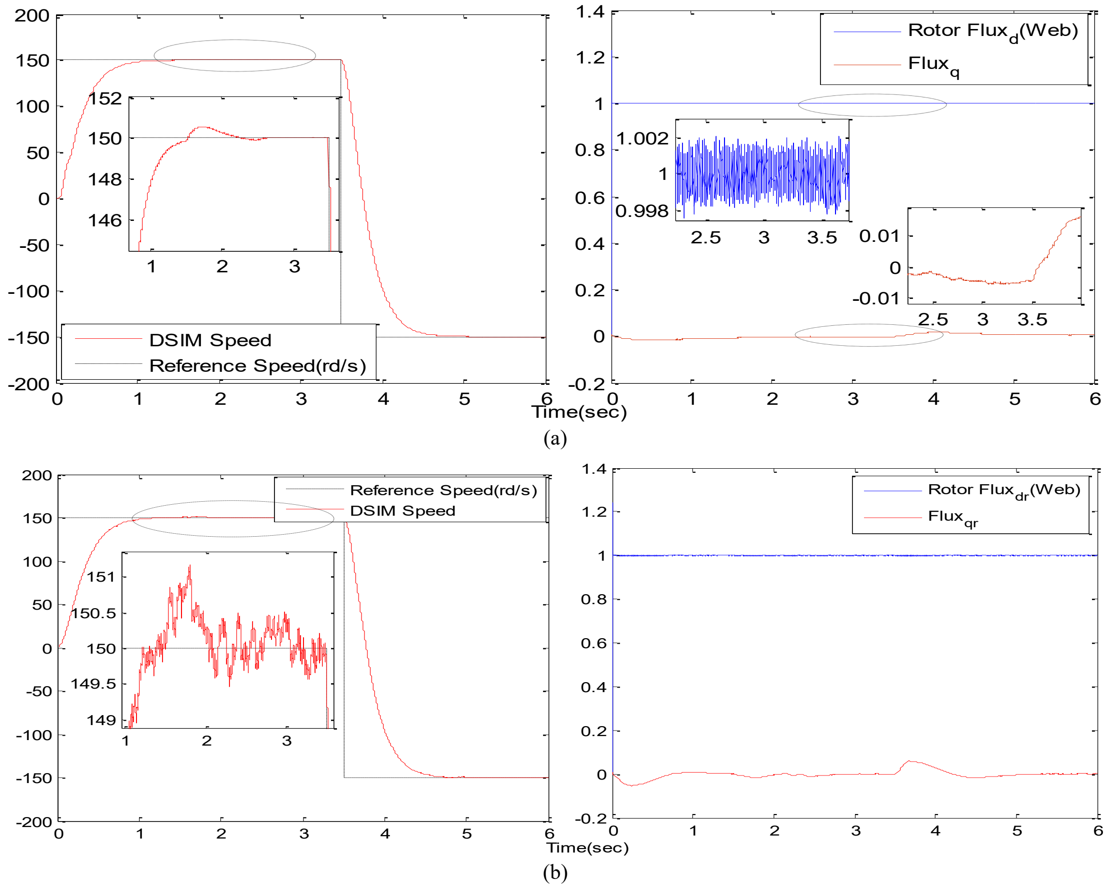


Fig. 10. Parameter variation of +100% J; for nominal speed test (a) proposed state observer (b) SM-MRAS estimator [32].

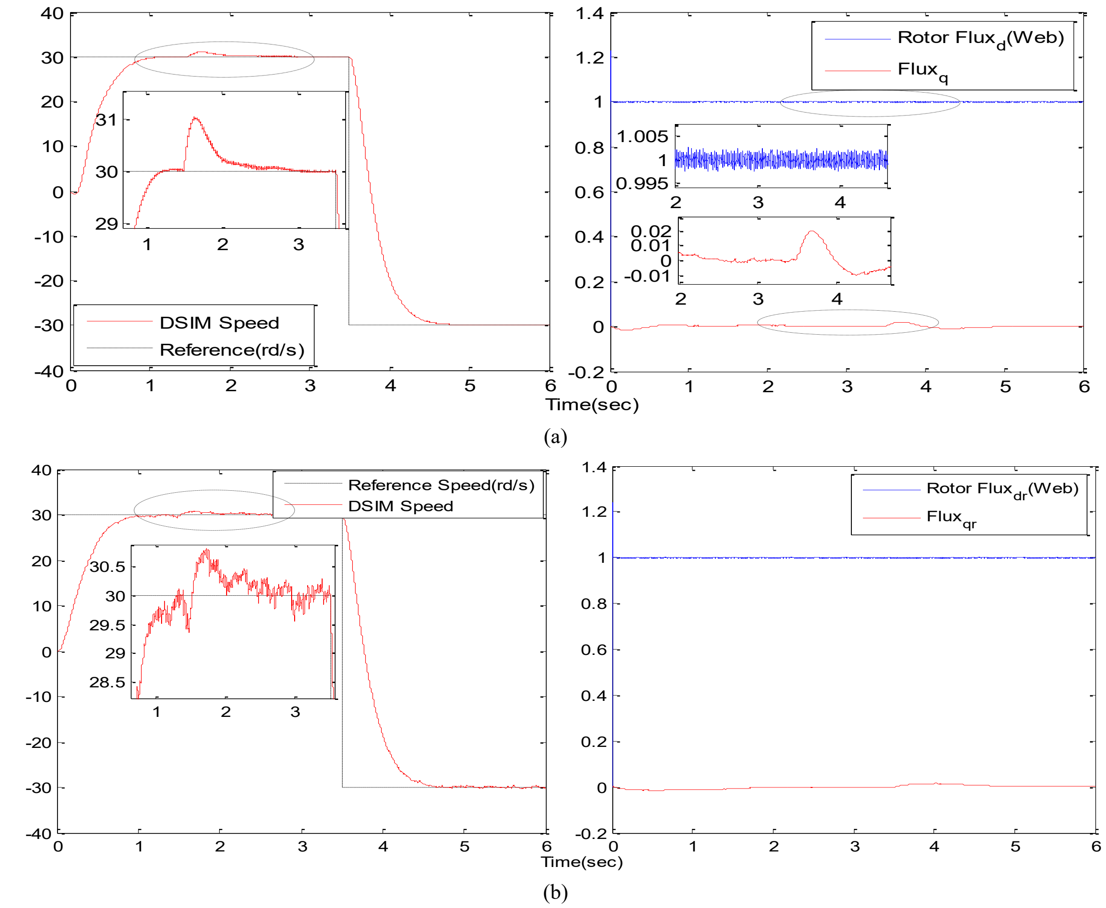


Fig. 11. Parameter variation of +100% J; for a low-speed test (a) proposed state observer (b) SM-MRAS estimator [32].

## REFERENCES


[1] E. E. Ward and H. Härer "Preliminary investigation of an invertor-fed 5-phase induction motor," Proc. IEE., vol. 116, no. 6, pp. 980–984, 1969.

[2] M. A. Mossa, H. Echeikh, A. Iqbal, T. Duc Do, and A. S. Al-Sumaiti, "A novel sensorless control for multiphase induction motor drives based on singularly perturbed sliding mode observer-experimental validation," Applied Sciences, vol. 10, no. 8, p. 2776, 2020.

[3] B. Ghalem, A. Bendiabdellah, "Six-Phase Matrix Converter Fed Double Star Induction Motor," Journal of Applied Sciences, ActaPolytechnicaHungarica, vol.7, no. 3, pp.163-176, 2010.

[4] M. A. Mossa, N. V. Quynh, H. Echeikh, and T. D. Do, "Deadbeat-Based Model Predictive Voltage Control for a Sensorless Five-Phase Induction Motor Drive," Mathematical Problems in Engineering, vol 2020, p. 4164526, 2020.

[5] F. Blaschke, "The principle of field orientation applied to the new trans-vector closed-loop control system for rotating field machines," Siemens-Review, vol. 39, pp. 217-220, 1972.

[6] M. A. Mossa and H. Echeikh, "A novel fault tolerant control approach based on backstepping controller for a five-phase induction motor drive: Experimental investigation," ISA Trans., vol. 112, pp. 373–385, 2021.

[7] M. A. Mossa, H. Echeikh, A. A. Z. Diab, H. Haes Alhelou, P. Siano, "Comparative Study of Hysteresis Controller, Resonant Controller and Direct Torque Control of Five-Phase IM under Open-Phase Fault Operation," Energies, vol. 14, p. 1317, 2021.

[8] M. A Mossa and A. A. Z. Diab, "Effective Model Predictive Control Approach for a Faulty Induction Motor Drive," International Review of Electrical Engineering (IREE), vol. 14, no. 5, pp. 314-327, 2019.

[9] M. Mossa, "Effective Predictive Flux Control for a Five Phase Induction Motor Drive with Inverter Output Filter," International Review of Electrical Engineering (IREE), vol. 13, no. 5, pp. 373-384, 2018.

[10] H. Khouidmi, A. Massoum and A. Meroufel, "Dual Star Induction Motor Drive: Modelling, Supplying and Control," International Journal of Electrical and Power Engineering, vol. 5, no. 1, pp. 28-34, 2011.

[11] P. Vas. "Sensorless Vector and Direct Torque Control," Oxford University Press, Oxford, 1998.

[12] R. Sadouni and A. Meroufel, "Indirect Rotor Field-oriented Control (IRFOC) of a Dual Star Induction Machine (DSIM) Using a Fuzzy Controller," Journal of Applied Sciences, ActaPolytechnicaHungarica, vol. 9, no. 4, pp177-192, 2012.

[13] M. Menaa, O. Touhami, R. Ibtiouen, and M. Fadel, "Sensorless direct vector control of an induction motor," Control Engineering Practice, vol. 16, no. 1, pp.67-77, 2008.

[14] R. Kianinezhad, B. Nahid-Mobarakeh, F. Betin, and G. A. Capolino, "Sensorless field-oriented control for six phase induction machines," Fourtieth IAS Annual Meeting. Conference Record of the 2005 Industry Applications Conference, pp. 999-1006, 2005.

[15] K. Marouani, K. Chakou, F. Khoucha, B. Tabache, and A. Kheloui, "Observation and Measurement of Magnetic Flux in a Dual Star Induction Machine," 19th Mediterranean Conference on Control and Automation, 2011, pp. 289-294.

[16] K. De Becker, K. Bernaerts, and S. Waldherr, "Luenberger observer design for a dynamic system with embedded linear program, applied to bioprocesses," IFAC-PapersOnLine, vol. 53, no. 2, pp. 15884-15891, 2020.

[17] P. Bernard, V. Andrieu, and D. Astolfi, "Observer design for continuous-time dynamical systems," Annual Reviews in Control, vol. 53, pp. 224-248, 2022.

[18] M. A. Mossa, H. Echeikh and A. Ma'arif, "Dynamic Performance Analysis of a Five-Phase PMSM Drive Using Two Different Sensorless Techniques," Journal of Robotics and Control (JRC), vol. 3, no. 3, pp. 289-308, 2022.

[19] Y. Zahraoui, M. Akherraz, and A. Ma'arif, "A comparative study of nonlinear schemes for induction motor operation improvement," International Journal of Robotics and Control Systems, vol. 2, no. 1, pp. 1-17, 2022.

[20] H. Kubota, K. Matsuse and T. Nakano, "DSP-based speed adaptive flux observer of induction motor," IEEE Transactions on Industry Applications, vol. 29, no. 2, pp. 344-348, March-April 1993.

[21] A. Benchaib, M. Tadjine, A. Rachid and A. Tayebi, "Adaptive sliding mode observer for state estimation of an induction motor on DSP-based system," 1997 IEEE International Electric Machines and Drives Conference Record, 1997, pp. MC2/3.1-MC2/3.3.

[22] A. K. Ali, and M. M. Mahmoud, "Reduced Order and Observer-Based Reset Control Systems with Time Delays," International Journal of Robotics and Control Systems, vol. 2, no. 3, pp.448-466, 2022.

[23] H. Khouidmi, A. Massoum, "Reduced-order Sliding Mode Observer Based Speed Sensorless Vector Control of Double Stator Induction Motor," Journal of Applied Sciences, Acta Poly technical Hungarica, vol. 11, no. 6, pp.229-249, 2014.

[24] R. Nilsen, M. P. Kazmierkowski, "Reduced-order observer with parameter adaptation for fast rotor flux estimation in induction machine," IEE Proceedings, vol. 136, no. 1, pp. 35-43, 1989.

[25] Zhong Peng, Z. Zheng, Y. Li, and Zicheng Liu, "Sensorless vector control of multiphase induction machine based on full-order observer and harmonic suppression," 2017 IEEE 3rd International Future Energy Electronics Conference and ECCE Asia (IFEEC 2017 - ECCE Asia), 2017, pp. 2153-2160.

[26] M. A. Mossa and S. Bolognani, "Effective model predictive current control for a sensorless IM drive," 2017 IEEE International Symposium on Sensorless Control for Electrical Drives (SLED), 2017, pp. 37-42.

[27] H. Echeikh, M. A. Mossa, N. V. Quynh, A. A. Ahmed, and H. H. Alhelou, "Enhancement of Induction Motor Dynamics Using a Novel Sensorless Predictive Control Algorithm," Energies, vol. 14, no. 14, p. 4377, 2021.

[28] M. A. Mossa, A. Saad Al-Sumaiti, T. Duc Do and A. A. Zaki Diab, "Cost-Effective Predictive Flux Control for a Sensorless Doubly Fed Induction Generator," IEEE Access, vol. 7, pp. 172606-172627, 2019.

[29] M. A. Mossa, "Effective predictive current control for a sensorless five-phase induction motor drive," Int. J. Power Electron, vol. 13, no. 4, pp. 502–532, 2021.

[30] M. A. Khoshhava, H. A. Zarchi, and G. A. Markadeh, "Sensor-less Speed and Flux Control of Dual Stator Winding Induction Motors Based on Super Twisting Sliding Mode Control," IEEE Transactions on Energy Conversion, vol. 36, no. 4, pp. 3231-3240, 2021.

[31] Z. Wu, O. Ojo, and G. Dong, "MRAS Speed Estimation and Full-Order Flux Observer for Dual Stator Winding Induction Motor Drives," 2007 IEEE Power Electronics Specialists Conference, 2007, pp. 2428-2434.

[32] H. Khouidmi, A. Benzouaoui, and B. Bessedik, "Sliding-mode MRAS Speed Estimator for Sensorless Vector Control of Double Stator Induction Motor," Majlesi Journal of Electrical Engineering, vol. 12, no. 3, pp. 41-53, 2018.